Monitoring the Aging Dynamics of Glycidyl Azide Polyurethane by NMR Relaxation Times

Mario Laviolette and Michèle Auger*

Département de Chimie, Centre de Recherche en Sciences et Ingénierie des Macromolécules, Université Laval, Québec, Québec, Canada G1K 7P4

Sylvain Désilets

Centre de Recherche pour la Défense Valcartier, 2459 boul. Pie-XI Nord, Val-Bélair, Québec, Canada G3J 1X5

Received September 1, 1998

ABSTRACT: We have used solid-state NMR to monitor the aging dynamics of a polyurethane based on glycidyl azide polymer (GAP) used as a binder in solid rocket propellants. We have shown by deuterium NMR longitudinal relaxation time (T_1) measurements that it is possible to monitor the degradation of the binder as a function of time for samples with different NCO/OH ratios. The longitudinal relaxation was found to be nonexponential. Thus, we have used a stretched exponential equation of the type Kohlrausch−Williams−Watts to determine the value of T_{1ww}. With the help of the gamma function, the average value of T_1 ($\langle T_1 \rangle$) was determined without knowing the shape of its distribution function. Since the solid-state NMR method has the advantage of being nondestructive, we were able to monitor the aging of the polyurethane samples that were kept in ambient conditions rather than in the extreme thermal conditions usually applied in aging studies of polymers.

Introduction

Conventional propellants use ammonium perchlorate aluminum as energetic oxidants and a polymeric binder made of hydroxy-terminated polybutadiene (HTPB). This oxidant mixture has the distinct disadvantage of producing large quantities of hydrochloric acid during combustion[1] (e.g., one space shuttle takeoff releases 220 tons of HCl in the atmosphere). We could call this a paradox when launching an environmental probe. Replacing ammonium perchlorate by another oxidant such as ammonium nitrate reduces to almost nothing the production of polluting agents during combustion. The down side to such substitution is a considerable drop in combustion energy.[2] This change in oxidant requires the development and characterization of energetic binders in order to compensate for the loss of energy during combustion.

Polyurethanes based on glycidyl azide polymer (GAP)[3] shown in Figure 1 are promising candidates as binders[4] in future low-smoke, low-pollution, and low-sensitivity solid rocket propellants.[5] Basically, a propellant is a mixture of an energetic solid and a plasticizer which is mechanically maintained by a polymeric binder. The integrity of the formulation is of primordial importance for the performance and the long-term stability of the propellant. Phenomena such as propellant degradation will change its properties over time and render it less effective, less safe, and sometime useless. The degradation of propellants is reflected by the decrease in its material content (plasticizer, stabilizer) and by the changes in the molecular weight or in the degree of cross-linking of the polymeric binder.

There is an increasing interest in the development of alternative methods to monitor degradation processes of polymeric binders in order to choose a propellant formulation with a low sensitivity to degradation.[6] Such techniques may help select the most resistant formulation in order to extend the time during which the material can perform its structural mission in a given environment. Accelerated degradation of polyurethane materials is mostly studied at moderate and elevated temperatures by using various approaches and techniques such as stabilizer depletion (high-performance liquid chromatography),[7] infrared spectroscopy,[8−10] gas evolution,[11] thermal behavior changes (differential scanning calorimetry,[10,12] thermogravimetric analysis,[13] microcalorimetry[14]), mechanical property changes (dynamic mechanical analysis,[15] stress−strain analysis[9]), solubility changes of polymers (soluble fraction), molecular weight, and cross-link density changes (gel permeation chromatography, swelling).[16] However, the extrapolation of the information measured at elevated temperatures does not always reflect the changes observed under normal conditions. In fact, the degradation of the material in use usually occurs at ambient temperature over a long exposure time. Techniques that would be sensitive to aging processes at ambient or moderate temperatures are strongly preferred to the ones using accelerated degradation procedures. The techniques mentioned above are very well-accepted techniques, but they also destroy the sample, thus preventing the study of the same sample over a period of time.

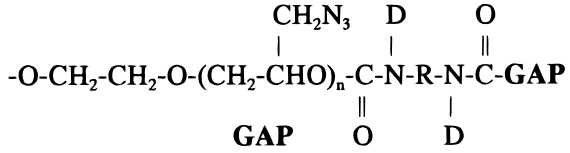

Figure 1. Representation of a section of a polyurethane based on glycidyl azide polymer (GAP) and isophorone diisocyanate (IPDI).

* To whom correspondence should be addressed. Phone 418-656-3393, Fax 418-656-7916, E-mail Michele.Auger@chm.ulaval.ca.

10.1021/ma981388+ CCC: $18.00
Published on Web 02/12/1999

We have used solid-state NMR to monitor the dynamic changes as a function of degradation time of a polymeric binder used in one of these new generation propellants. The studied binder is a GAP (glycidyl azide polymer)−IPDI (isophorone diisocyanate)-based polyurethane. Such experiments were performed by monitoring the variation of the proton spin−lattice relaxation times in the rotating frame (H $T_{1\rho}$) measured from ^{13}C spectra for different NCO/OH ratios in the polyurethane binder and by monitoring the variation of the deuterium longitudinal relaxation time (^2H T_1) of deuterated polyurethane as a function of the aging time. The aim of this paper is to evaluate the potential of NMR relaxation time measurements to investigate the integrity of the GAP−IPDI-based polyurethane binder exposed to aging treatments. We will also demonstrate the use of the Kohlrausch−Williams−Watts (KWW) stretched exponential and gamma functions to determine the value of the average longitudinal relaxation times in the polyurethane systems.

Theory

Nonexponential Longitudinal Relaxation Time. Relaxation phenomena in polymers determined by various methods, such as dielectric relaxation, photon correlation spectroscopy, and mechanical relaxation experiments, have been shown to be strongly nonexponential. In most cases, the relaxation behavior cannot be adequately fitted by a single exponential or by a superposition of two or three exponentials but is better described by a stretched exponential such as the Kohlrausch−Williams−Watts function shown in eq 1:[17−19]

$$M = M_0\left(1 - A\exp\left[-\left(\frac{\tau}{T_{1ww}}\right)^{\beta}\right]\right) \tag{1}$$

where M is the z magnetization at a variable delay time τ, M_0 is the equilibrium magnetization, A is a preexponential weighting factor related to the extent of inversion in the inversion−recovery experiment, β is the stretch parameter (with $0 < \beta \leq 1$), and T_{1ww} is the longitudinal relaxation time. The stretch parameter β is directly related to the distribution of T_{1ww} values. For instance, a value of $\beta = 1$ reflects an infinitely narrow distribution (in such case eq 1 becomes a single exponential), and a value of $\beta = 0$ reflects an infinitely broad distribution. In most systems, it has not been possible to clarify the precise nature of this nonexponential behavior by means of simple experiments. The most commonly proposed explanations[19−21] are either a spatially heterogeneous distribution of correlation times where slow and fast processes occur at the same time or an intrinsically nonexponential loss of correlation in a homogeneous system where slow and fast processes occur in series.

The use of the KWW stretched exponential is well documented in the literature in the field of dielectric relaxation spectroscopy (DRS)[22] but has been very little exploited in the field of NMR spectroscopy and even less in the field of polymer NMR.[23] The stretched exponential function has the advantage of having fewer parameters to fit compared to the multiexponential functions commonly used in solids.

If a relaxation function is considered as arising from a superposition of exponential relaxation functions, it can be well approximated by the following KWW relation:

$$\phi(\tau) = \int_0^\infty e^{-\tau/T}\rho(T)\,dT \approx e^{-(\tau/\tilde{T})^{\beta}} \tag{2}$$

Equation 2, along with the normalization condition $\int_0^\infty \rho(T)\,dT = 1$, defines the relaxation time distribution function ρ(T). Lindsey and Patterson[20] have shown for the field of dielectric relaxation spectroscopy that it is possible to obtain the average value of the relaxation time $\langle T\rangle$ without knowing the shape of the relaxation time distribution function $\rho(T)$. We have applied this to our NMR relaxation time measurements. The following summarizes the mathematics behind the equations. For further reading, we refer to the article mentioned above.[20]

The moment of the average value of the relaxation time distribution $\langle T^n\rangle$ can be expressed in terms of the relaxation function $\phi(\tau)$ by

$$\langle T^n\rangle = \int_0^\infty T^n\rho(T)\,dT = \frac{1}{\Gamma_{(n)}}\int_0^\infty \tau^{n-1}[\phi(\tau)]\,d\tau \tag{3}$$

where $\Gamma_{(n)}$ is the gamma function and is represented by $\int_0^\infty \tau^{n-1}e^{-\tau}\,d\tau$, and $\phi(\tau)$ is the exponential relaxation function defined in eq 2. To demonstrate this, we have rewritten eq 3 using eq 2 and interchanged the order of integration. We therefore obtain

$$\langle T^n\rangle = \frac{1}{\Gamma_{(n)}}\int_0^\infty \tau^{n-1}\left[\int_0^\infty e^{-\tau/T}\rho(T)\,dT\right]d\tau = \frac{1}{\Gamma_{(n)}}\int_0^\infty \rho(T)\left[\int_0^\infty \tau^{n-1}e^{-\tau/T}\,d\tau\right]dT$$

$$\langle T^n\rangle = \frac{1}{\Gamma_{(n)}}\int_0^\infty \rho(T)[\Gamma_{(n)}T^n]\,dT$$

$$\langle T^n\rangle = \int_0^\infty T^n\rho(T)\,dT$$

which is the definition of $\langle T^n\rangle$.

To determine the average value of the relaxation time distribution $\langle T^n\rangle$ from experimental results, eq 3 can be written using the definition of eq 2 as

$$\langle T^n\rangle = \frac{1}{\Gamma_{(n)}}\int_0^\infty \tau^{n-1}e^{-(\tau/\tilde{T})^{\beta}}\,d\tau \tag{4}$$

With

$$\upsilon = \left(\frac{\tau}{\tilde{T}}\right)^{\beta} = \tau^{\beta}\tilde{T}^{-\beta} \quad \frac{d\upsilon}{d\tau} = \tilde{T}^{-\beta}\beta\tau^{\beta-1} \quad d\tau = \tilde{T}\beta^{-1}\upsilon^{1/\beta-1}\,d\upsilon$$

$$\tau = \upsilon^{1/\beta}\tilde{T}$$

Equation 4 may be rewritten as

$$\langle T^n\rangle = \frac{1}{\Gamma_{(n)}}\int_0^\infty \tilde{T}^{n-1}\upsilon^{(n-1)/\beta}e^{-\upsilon}\tilde{T}\beta^{-1}\upsilon^{1/\beta-1}\,d\upsilon = \frac{\tilde{T}^n\beta^{-1}}{\Gamma_{(n)}}\int_0^\infty \upsilon^{(n/\beta)-1}e^{-\upsilon}\,d\upsilon$$

which simplifies to

$$\langle T^n\rangle = \left(\frac{\tilde{T}^n}{\beta}\right)\left(\frac{\Gamma_{(n/\beta)}}{\Gamma_{(n)}}\right) \tag{5}$$

For the first moment, which is analogous to the center of gravity of the distribution, $n = 1$, and the average value of the relaxation correlation time distribution is given by

$$\langle T^n \rangle = \left(\frac{\tilde{T}}{\beta}\right)\Gamma_{(1/\beta)} \tag{6}$$

where $\tilde{T}$ (T_{1ww}) and β are the fitting parameters obtained by fitting our experimental data with eq 1, and the value of $\Gamma_{(1/\beta)}$ is defined in handbook tables.

Materials and Methods

Sample Preparation. Polyurethane elastomers based on GAP−IPDI were prepared by using a procedure described in the literature.[24] The samples used for the ^{13}C solid-state NMR studies were precisely cut to the dimensions of the NMR sample tubes using a drill press.

Samples of deuterated GAP−IPDI-based polyurethanes with different NCO/OH ratios were prepared at the Defence Research Establishment Valcartier (DREV), Québec, Canada, by the following procedure. First, the hydroxyl functions of GAP were deuterated using 20 g of a mixture of GAP diol/triol (95:5) purchased from Rocketdyne Co. (Canoga Park, CA) dissolved in 200 mL of dry THF. A 1.2 g sample of pure NaH purchased from Aldrich Chemical Inc. (Milwaukee, WI) was carefully added to the GAP solution. The mixture was kept under a dry nitrogen atmosphere at 68 °C for 3 h. The resulting solution was brought to room temperature, followed by the addition of 20 mL of D_2O, and kept overnight at room temperature. $MgSO_4$ was added to dry the deuterated polymer, followed by filtration and evaporation of THF under vacuum overnight at 50 °C. The deuterated polymer was kept dry in a desiccator containing calcium chloride. The water content of the deuterated GAP−OD polymer was below 150 ppm as determined by Karl Fisher (1−2% of the total ^2H NMR signal). The amount of deuterium present in the polymer was also verified using ^2H NMR spectroscopy of the polymer in chloroform. The signal was identified to be GAP−OD (and not D_2O) by comparison with a ^2H NMR spectrum of the polymer with a known added quantity of D_2O.

Four samples of deuterated GAP−IPDI polyurethane were prepared at DREV using the deuterated GAP−OD polymer in which a 80:20 mixture of isophorone diisocyanate (IPDI): trifunctional N-100 isocyanate was added at the NCO/OH ratios of 0.8, 1.0, 1.2, and 1.4. The alcohol equivalent weight (EW) used for the ratio calculations were of EW = 1210 g/mol for the GAP diol and EW = 1180 g/mol for the GAP triol. Dibutyl tin dilauriate (DBTDL) was added at 0.01% to accelerate the curing process. The curing of the polyurethanes was done at 50 °C under dry conditions and was considered completed after 8 days, as determined previously.[24]

Samples were kept sealed in a desiccator and aged in daylight conditions at room temperature from 0 to 52 weeks. The sample identified as 7 months (aged) has been aged in the absence of daylight at 80 °C for 7 months. For further reading on the reaction of the GAP prepolymer and the diisocyanate IPDI, we refer to ref 24.

NMR Experiments. The ^{13}C solid-state NMR magic angle spinning (MAS) and the ^2H NMR static spectra of GAP−IPDI polyurethane were acquired with a Bruker ASX 300 solid-state NMR spectrometer (Bruker Canada Ltd., Milton, Ontario) operating at a frequency of 75.44 and 46.05 MHz for ^{13}C and ^2H, respectively. A broad-band/^1H dual frequency 7 mm MAS probehead was used for all ^{13}C experiments and was purchased from Bruker (Bruker Canada Ltd., Milton, Ontario). The ^2H NMR spectra were acquired using a static single frequency 10 mm probehead, also purchased from Bruker.

The ^{13}C spectra were acquired using a cross-polarization (CP) pulse sequence[25] with high power proton decoupling during acquisition. The spectra were acquired at 30, 50, and 70 °C, and the optimal contact times for the CP experiment at these temperatures were determined to be 1, 6, and 10 ms, respectively. The sample was spun at the magic angle at a rate of 4 kHz. The ^1H $\pi/2$ pulse length was typically 5.0 μs, corresponding to a rotating-frame frequency of 43 kHz, and the recycle delay was set to 5.0 s. Between 12 000 and 15 000 transients were recorded with 4096 points, and a spectral width of 50 kHz was used for each spectra. The H $T_{1\rho}$ measurements were done using 11 different time increments varying between 400 μs and 6 ms. For the H $T_{1\rho}$ measurements, the number of transients was limited to 1600. During processing, the FID were zero-filled to 8192 points and submitted to a 100 Hz line broadening.

The ^2H NMR spectra were recorded using the basic quadrupolar echo sequence,[26] and T_1 values were obtained using the inversion recovery sequence. T_1 were measured at temperatures between 20 and 75 °C at regular intervals to obtain good T_1 vs temperature curves. Each T_1 relaxation time value was obtained using 20 relaxation delays varying from 10 μs to 300 ms. The $\pi/2$ pulse length was typically 6.0 μs, and the recycle delay was 200 ms. Between 1300 and 1600 transients were recorded with 4096 points and a spectral width of 250 kHz for each spectrum. During processing, the FID were submitted to a 500 Hz line broadening.

Mathematical Treatment and Data Fitting. Relaxation times (T_1) and stretch parameters (β) for each sample at different temperatures were obtained by fitting the nonexponential relaxation curve data with the KWW equation (eq 1) using the spreadsheet program Excel and minimizing the root-mean-square difference (rmsd) between the experimental and the fitted data. The minimization for each data set was done using 100 different sets of initial fitting parameters that were randomly generated. Only the fit with the lowest rmsd was kept for data analysis and was assumed to be the absolute minimum.

Figure 2A presents a comparison of a GAP−IPDI-based polyurethane T_1 relaxation curve fitted with a single-exponential and nonexponential (KWW) function. The value of T_1 obtained using the KWW equation will be denoted as T_{1ww} for the rest of this paper. The value of T_{1ww} represents a value near or at the maximum of an asymmetric Kolrausch−Williams−Watts distribution that is dependent on the width of the distribution, i.e., dependent on the value of β.[17,18] Since the shape and/or width of the distribution may vary as a function of temperature, the use of the T_{1ww} value to monitor the T_1 vs temperature is not appropriate. In addition, since the value of T_{1ww} cannot be assumed to represent the precise value of this maximum of the distribution function, it is more appropriate to use the first moment of this distribution instead, i.e., the average value of the $\langle T_1 \rangle$ distribution. We have used eq 6, which applies the use of gamma functions and the value of β, to translate the T_{1ww} value into the first moment, i.e., the average value $\langle T_1 \rangle$ of the relaxation distribution. This method ensures that we are always plotting an absolute value of T_1 vs temperature. The value of $\langle T_1 \rangle$ therefore represents the average of the distribution instead of a nonabsolute value that represents the region of the maximum. Figure 2B presents an example of the T_1 vs temperature curve obtained using $\langle T_1 \rangle$ compared to T_{1ww}.

Results and Discussion

^{13}C CPMAS Solid-State NMR Spectroscopy. Figure 3 presents the ^{13}C CPMAS solid-state NMR spectrum of a GAP−IPDI-based polyurethane sample with a NCO/OH ratio of 1.2 at 50 °C. Several spectra were acquired at temperatures of 30, 50, and 70 °C for samples with NCO/OH ratios of 1.0, 1.2, and 1.4. The cross-polarization contact times were optimized for each ratio at different temperatures and were found to be 1, 6, and 10 ms at 30, 50, and 70 °C, respectively. There was no significant observable difference in the shape or width of the spectral features for the different NCO/OH ratios. Three major peaks are present in the spectra at 51.7, 69.6, and 78.6 ppm. These peaks are respectively attributed to the CH_2N_3, CH_2O, and CHO func-

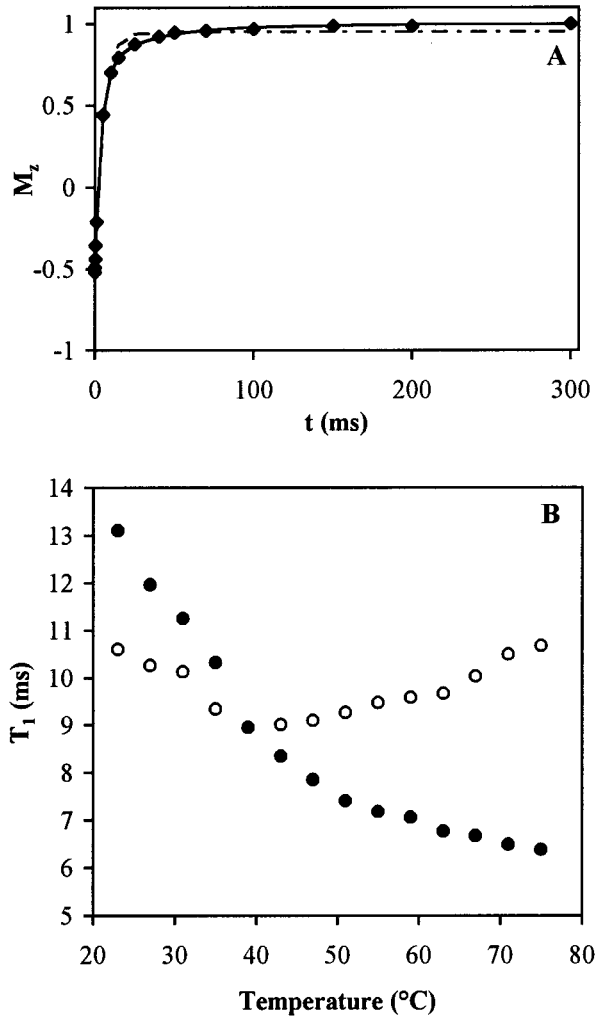

Figure 2. (A) Magnetization relaxation data (◆) for a polyurethane sample with a NCO/OH ratio of 0.8 at 70 °C fitted with a monoexponential (dotted line) and a KWW type stretched exponential (solid line). (B) Comparison between using T_{1ww} (○) vs the first moment of the distribution $\langle T_1 \rangle$ (●) when plotting the magnetization longitudinal relaxation time (T_1) vs temperature curves for a sample of GAP−IPDI-based polyurethane with a NCO/OH ratio of 1.4 that was aged for 28 weeks at 80 °C.

tions of the GAP polymer, as described in the literature.[24] There are also several peaks in the 20−45 ppm region corresponding to the IPDI moiety and a peak at 155.6 ppm corresponding to the C═O of the urethane functions.[24]

Spin−Lattice Relaxation in the Rotating Frame (H $T_{1\rho}$). Relaxation times are sensitive to the spectral density of molecular dynamics with rates in the order of the characteristic frequency $\omega_r = \gamma B_r$,[19,27] where B_r denotes the strength of the relevant B field. For the longitudinal relaxation time in the laboratory frame (T_1), this is the B_0 field while for the longitudinal relaxation time in the rotating frame ($T_{1\rho}$), this is the B_1 field used to spin lock the magnetization. Thus, T_1 probes the spectral density at the Larmor frequency (10^7-10^8 s^{-1}) while $T_{1\rho}$ is sensitive to slower motions with rates between 10^3 and 10^5 s^{-1}. The value of the corresponding relaxation time is minimum when the rate of the motion is approximately equal to the characteristic frequency γB_r. This can be seen as the result of a resonant coupling of the local fluctuating fields with the spin system, which accelerates the return to the Boltzmann equilibrium.[19]

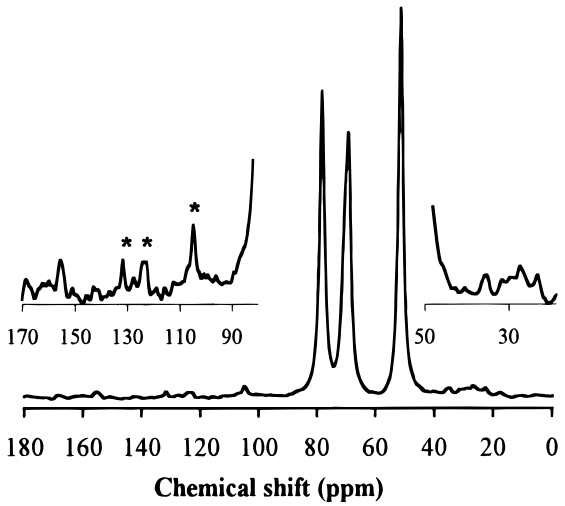

Figure 3. Solid-state ^{13}C MAS NMR spectrum of GAP−IPDI polyurethane at a NCO/OH ratio of 1.2. The spectrum was recorded at a temperature of 50 °C with a contact time of 6 ms. The insets show the expanded spectral region of IPDI signals between 20 and 50 ppm and the presence of urethane at 155.6 ppm. The spinning sidebands are indicated by asterisks.

Table 1. H $T_{1\rho}$ Values (in ms) for the Three Major Components (CH_2N_3, CHO, and CH_2O) of the ^{13}C Solid-State NMR Spectra of a GAP−IPDI-Based Polyurethane for Three Different NCO/OH Ratios, 1.0, 1.2, and 1.4 at 30, 50, and 70 °C

temp, °C	NCO/OH 1.0	NCO/OH 1.2	NCO/OH 1.4
		CH_2N_3	
30	1.8	1.1	1.7
50	5.7	5.3	7.7
70	9.8	6.4	12.6
		CHO	
30	1.4	0.8	1.1
50	4.9	4.1	6.2
70	10.0	4.8	9.9
		CH_2O	
30	1.9	1.2	1.8
50	6.2	4.4	7.9
70	8.4	6.0	10.7

For monitoring polymer degradation, the most interesting part of the ^{13}C NMR solid-state MAS spectrum of the GAP−IPDI-based polyurethane sample (Figure 3) would be the C═O region, but unfortunately, the resolution and signal-to-noise ratio of the peak at 155.6 ppm are not sufficient for relaxation measurements.[24] Moreover, due to the weak natural abundance of the ^{13}C nuclei, the acquisition of ^{13}C solid-state NMR spectra is too lengthy for a thorough analysis of the aging dynamics based on the C═O signal measurement. However, we have measured the H $T_{1\rho}$ of the three major components, i.e., the CH_2N_3, CH_2O, and CHO functions, as a function of temperature. These functions are all representative of the polymer soft segments. The H $T_{1\rho}$ was chosen over the ^{13}C $T_{1\rho}$ since the values of the proton $T_{1\rho}$ are much shorter, thus allowing the measurement of the relaxation times at more than one temperature for each sample.

Table 1 shows the H $T_{1\rho}$ results obtained for three different NCO/OH ratios, 1.0, 1.2, and 1.4, each measured at 30, 50, and 70 °C. These results first indicate that for each sample the values of the H $T_{1\rho}$ increase with temperature, indicating that the systems are in the extreme narrowing limit (high-temperature side) of the T_1 vs temperature curve. This is expected consider-

ing that the B_1 field used in the $T_{1\rho}$ experiments is much smaller than the external magnetic field (B_0).

The sample with a NCO/OH ratio of 1.2 has the minimum value of H $T_{1\rho}$ relaxation time, at all temperatures studied, suggesting at first glance a higher rigidity. Mechanical property measurements done at DREV[28] have shown the sample with a NCO/OH ratio of 1.2 to have the highest rigidity compared to the 1.0 and 1.4 ratio samples. This can be explained by the formation of long urethane chains combined with the presence of a good level of cross-linking. In the 1.0 ratio sample, the reticulation degree is lower due to the smaller number of isocyanate functions available to form reticulations, which causes the sample to have longer chains and less reticulation. In the 1.4 ratio sample, the higher number of isocyanate functions available results in the formation of shorter linear urethane chains and the formation of smaller molecules such as allophanates, urea, and biuret.[24] These smaller molecules may cause swelling in the polyurethane, thus decreasing the overall rigidity of the 1.4 ratio sample compared to the 1.2 ratio sample.

As mentioned above, the results obtained with the three samples suggest that the decrease in the H $T_{1\rho}$ values observed at the three temperatures investigated is indicative of a higher rigidity of the 1.2 ratio sample, reflected by slower motions in the kilohertz motional regime. However, the relation between the changes in relaxation times and molecular dynamics ideally requires the study of the variation of the minimum value of the T_1 vs temperature curve instead of using a single T_1 value at a given temperature. Due to a multitude of experimental restrictions, it is not always possible to obtain the minimum value. However, partial segments of the curve can be sufficient if the monitored data are on the low-temperature side of the curve since changes in the amplitude and frequency of molecular motion are both reflected in the same manner on the T_1 variation. For example, a higher frequency and a higher amplitude of molecular motion will both cause a reduction of the T_1 value. However, data on the high-temperature side (extreme narrowing limit) of the curve cannot usually be properly interpreted without the value of the T_1 minimum since changes in the frequency and amplitude of molecular motion will modify the T_1 value in opposite ways.

Due to the long time required to measure one relaxation time from ^{13}C spectra at a given temperature, the acquisition of many points to construct a typical T_1 vs temperature curve was too time-consuming for the spectrometer availability. For example, due to the long recycle delay (5 s), a typical $T_{1\rho}$ measurement with 11 time increments took just over a day (~25 h). Consequently, it was not practical for degradation studies to acquire several T_1 vs temperature curves as a function of aging time for a given sample. For this reason, we chose to use deuterated samples of our binder in order to monitor the variation of the ^2H spin−lattice relaxation as a function of the aging time. The use of ^2H T_1 considerably shortens the experimental time (due to efficient quadrupolar relaxation), permitting to probe the sample in a more extensive manner.

^{2}H Spin−Lattice Relaxation Measurements (^{2}H T_1). Figure 4 shows the solid-state ^2H spectrum of an amorphous GAP−IPDI polyurethane sample with a NCO/OH ratio of 1.4 acquired at 20 °C. The spectrum is typically isotropic due to the high degree of motion

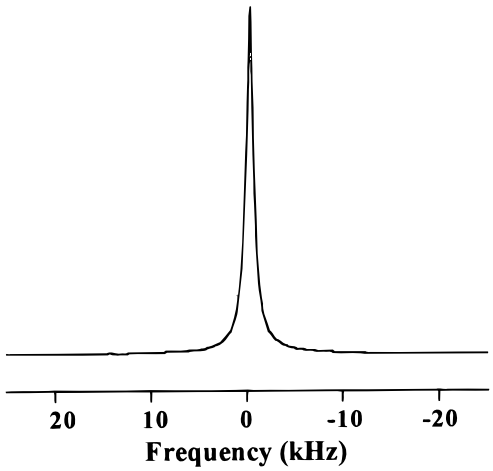

Figure 4. Solid-state ^2H NMR spectrum of GAP−IPDI polyurethane at a NCO/OH ratio of 0.8. The spectrum was recorded at 20 °C.

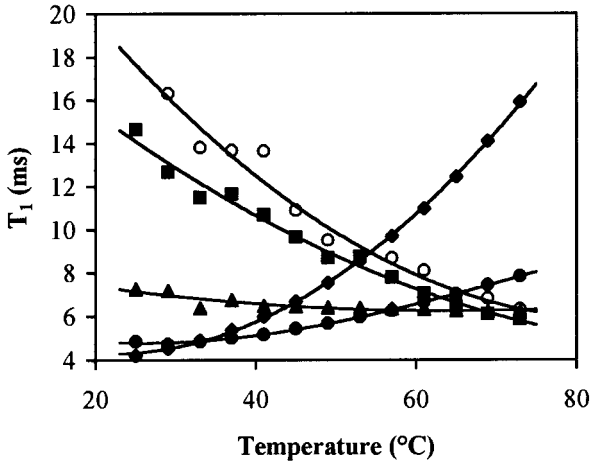

Figure 5. $\langle T_1 \rangle$ vs temperature curves obtained for samples of unaged GAP−IPDI polyurethane at varying NCO/OH ratios. The different ratios are pure GAP−OH prepolymer: (◆), 0.8 (●), 1.0 (▲), 1.2 (○), and 1.4 (■).

common for polymers at temperatures above their glass transition temperature (−41 °C for GAP−IPDI polyurethane). Figure 5 shows the variation of the $\langle T_1 \rangle$ values for different samples with NCO/OH ratios of 0.8, 1.0, 1.2, and 1.4 and for a sample of deuterated hydroxy-terminated glycidyl azide polymer (GAP−OD) monitored between 20 and 75 °C.

As mentioned above, the minimum value of $\langle T_1 \rangle$ in amorphous polymers is reached at a temperature when molecular motions are occurring at a frequency close to the Larmor frequency, i.e., 4.5×10^7 s^{-1} in a 7.04 T magnetic field. This value increases at temperatures below and above this minimum. Therefore, a variation of the overall position of the $\langle T_1 \rangle$ vs temperature curve is expected as a function of the mechanical properties of the various samples. The results presented in Figure 5 show that, for the temperature range studied, the relaxation time values for the deuterated hydroxy-terminated glycidyl azide prepolymer (GAP−OD) are representative of the high-temperature side (extreme narrowing limit) of the curve and that molecular motions on the order of the Larmor frequency occur at temperatures between 15 and 25 °C. When mixing this prepolymer with the isocyanate to form the urethane link, a gradual shift of the curve is observed in the temperature range studied, from the high-temperature

side of the $\langle T_1 \rangle$ curve toward the low-temperature side as the NCO/OH ratio increases. This is representative of an increasing rigidity in the sample with an increasing NCO/OH ratio. More specifically, the results indicate that, by increasing the NCO/OH ratio, the minimum value of $\langle T_1 \rangle$ shifts toward higher temperatures, which means that more energy is required in order to observe molecular motions with rates close to the Larmor frequency. More specifically, in the sample with a NCO/OH ratio of 0.8, molecular motions in the 4.5×10^7 s^{-1} range are observed at temperatures of about 30−35 °C compared the same rates occurring at a temperature above 75 °C for the 1.4 NCO/OH ratio sample.

Molecular dynamics is reflected not only on the T_1 vs temperature curve by a right or left shift of the minimum as a function of temperature but also by an increase or a decrease of the minimum T_1 value at a given temperature. This is characteristic of the amplitude of the motion, with higher T_1 values being associated to motions with lower amplitude. The results presented in Figure 5 indicate that the maximum values of $\langle T_1 \rangle$ are obtained for the 1.2 ratio curve. This is indicative of a higher rigidity for the 1.2 ratio sample, as also found by mechanical property studies and by the H $T_{1\rho}$ measurements (see previous section).

The variations of the $\langle T_1 \rangle$ vs temperature curves were monitored as a function of aging time for two different samples at NCO/OH ratios of 0.8 and 1.4. Figure 6a shows the variation of the $\langle T_1 \rangle$ vs temperature curve (recorded between 20 and 75 °C) for five different aging times of the GAP−IPDI polyurethane sample with a NCO/OH ratio of 0.8. As the sample ages, no significant change is observed in the temperature of the minimum $\langle T_1 \rangle$ value, but a significant increase of the overall value of the curve is obtained. This decrease in relaxation efficiency is indicative of a decrease in the amplitude of motion, thus indicating an increasing rigidity of the sample over time.

The reproducibility of the experiments is reflected by the two curves acquired 1 day apart on the same sample (6 months) (Figure 6A). On the other hand, there is no change in the $\langle T_1 \rangle$ curves between 6 months and 1 year. Figure 6B presents the variation of the $\langle T_1 \rangle$ relaxation values at 30 °C ($\langle T_1 \rangle$ minimum) as a function of the aging time for the sample with a NCO/OH ratio of 0.8. These results indicate that the value of the relaxation time, at the minimum of the $\langle T_1 \rangle$ vs temperature curve, is constant after about 25 weeks. This suggests that the process giving rise to the changes in $\langle T_1 \rangle$ is most likely the stabilization of the polymer rather than degradation. It would therefore be necessary to investigate this sample over a longer time period in order to visualize any changes due to polymer degradation.

Using the KWW equation to obtain the relaxation times allows also the determination of the value of the β stretch parameter. This parameter is indicative of the width of the relaxation time distribution. Probing this value as a function of temperature is related to the variation of the overall sample as a function of temperature and also as a function of aging time. Figure 6C shows both of these variations for the 0.8 ratio sample. The results show no significant variation as a function of aging time, indicating that the variation in molecular motion observed in the $\langle T_1 \rangle$ measurements is homogeneous throughout the sample. This suggests that the formation of different density regions in the polymer over time, which is expected during degradation due to a decreased molecular weight, seems to be absent for this sample. This homogeneous variation of $\langle T_1 \rangle$ is therefore probably more characteristic of polymer stabilization rather than polymer degradation. On the other hand, the results presented in Figure 6C also

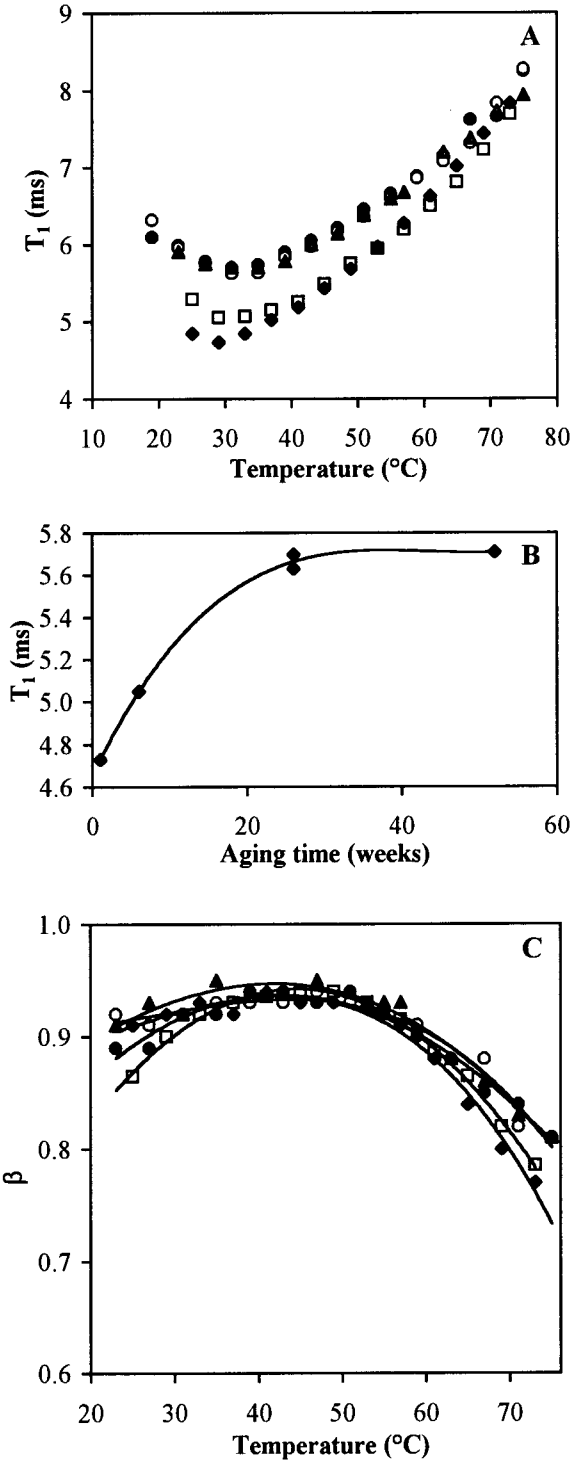

Figure 6. (A) $\langle T_1 \rangle$ vs temperature curves for a sample of GAP−IPDI polyurethane with a NCO/OH ratio of 0.8 at different aging times. The curves presented here are for a sample aged for 3 days (◆), 6 weeks (□), 6 months (●, ○) and 1 year (▲). (B) Variation of the value of $\langle T_1 \rangle$ at 30 °C for the sample of GAP−IPDI polyurethane at a NCO/OH ratio of 0.8 as a function of aging time. (C) Variation of the stretch parameter β as a function of temperature for different aging times for the sample of GAP−IPDI polyurethane at NCO/OH ratio of 0.8. The curves presented here are for a sample aged for 3 days (◆), 6 weeks (□), 6 months (●, ○), and 1 year (▲).

indicate a considerable change in the value of β as a function of temperature for a given aging time, with an increasing width of the relaxation time distribution at temperatures above 50 °C.

Figure 7A presents the variation of the $\langle T_1 \rangle$ vs temperature curves as a function of aging time for the GAP−IPDI polyurethane sample at a NCO/OH ratio of 1.4. It can be seen that the overall $\langle T_1 \rangle$ vs temperature curve decreases as a function of aging time. Since this is on the low-temperature side of the $\langle T_1 \rangle$ minimum, these results indicate that the system is becoming less rigid due to an increase in the rate and/or amplitude of motion. The sample named "7 months (aged)" is a sample that was aged at 80 °C for a period of 7 months. It has attained a similar rigidity as the sample that was aged at ambient conditions for 1 year. Figure 7B presents the variation of the $\langle T_1 \rangle$ relaxation values recorded at 53 and 74 °C as a function of aging time for the sample at a NCO/OH ration of 1.4. For both these temperatures, the value of the relaxation time continues to decrease after about 50 weeks, indicating a decreasing rigidity of the polymer, thus reflecting polymer degradation.

The variation of the stretched exponential coefficient (β) for the 1.4 ratio sample, presented in Figure 7C, indicates that there are significant differences as the sample ages. More specifically, the width of the relaxation time distribution increases at temperatures below 40° as a function of the aging time of the sample, indicating an increasing heterogeneity of the sample. Combined with the results obtained from the $\langle T_1 \rangle$ vs temperature curves, these results indicate that the sample is changing in a nonhomogeneous fashion throughout the polymeric matrix as a function of aging time. This is characteristic of polymer degradation due to a decrease of the polymer network, thus reflecting a decreasing rigidity.

It is interesting to note that the variation of the stretch parameter β for the sample after 1 year is different from the sample that was aged at very high temperature (80 °C) for 7 months, while for the same samples, there is no significant difference in the $\langle T_1 \rangle$ vs temperature curves. Both samples have the same range of molecular motions ($\langle T_1 \rangle$ vs temperature) but are different in terms of molecular density (β vs temperature). These results suggest that accelerated aging by very high temperatures is different from the room-temperature aging process. This is characteristic of different aging processes for the various functions present (urethane, urea, alophanate, biuret) in the polyurethane with the NCO/OH ratio of 1.4. It is suspected that the aging at room temperature resulted more from a photolysis process while the accelerated aging in the dark at 80 °C (7 months) was more the result of a hydrolysis or a thermolysis process.[29] Finally, the variation of the value of β as a function of temperature at a given aging time indicates that as the system gains energy, the width of the distribution of relaxation times starts decreasing.

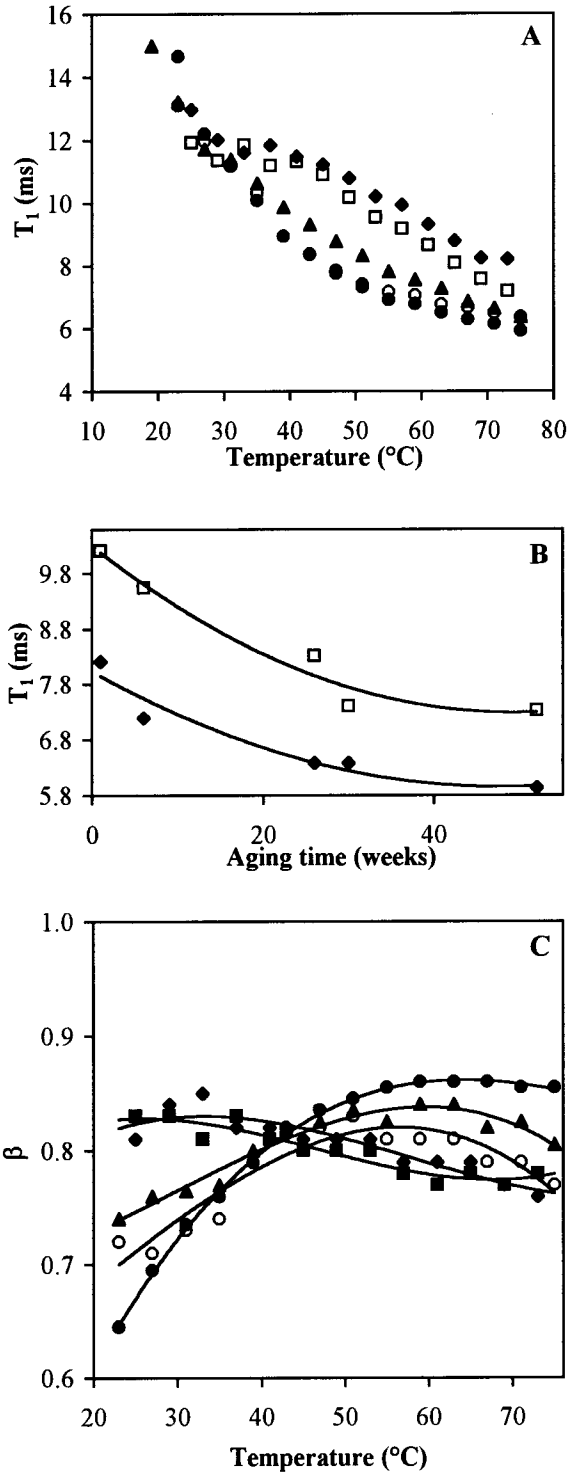

Figure 7. (A) $\langle T_1 \rangle$ vs temperature curves for a sample of GAP−IPDI polyurethane with a NCO/OH ratio of 1.4 at different aging times. The curves presented here are for a sample aged for 3 days (◆), 6 weeks (□), 6 months (▲), and 1 year (●) and for a sample that was aged at 80 °C for 7 months (○). (B) Variation of the value of $\langle T_1 \rangle$ at 53 °C (□) and 74 °C (◆) for the sample of GAP−IPDI polyurethane with a NCO/OH ratio of 1.4 as a function of aging time. (C) Variation of the stretch parameter β as a function of temperature for different aging times for the sample of GAP−IPDI polyurethane with a NCO/OH ratio of 1.4. The curves presented here are for a sample aged for 3 days (◆), 6 weeks (■), 6 months (▲), and 1 year (●) and for a sample that was aged at 80 °C for 7 months (○).

Conclusions

We have monitored in the present study the aging dynamics of a glycidyl azide polyurethane as a function of the NCO/OH ratio. The ^{13}C NMR H $T_{1\rho}$ results suggest a higher rigidity in the soft segment (GAP extended chains) of the GAP−IPDI polyurethane with a NCO/OH ratio of 1.2 while the ^{2}H NMR T_1 measurements indicate a higher rigidity in the hard segment (urethane function) of the GAP−IPDI polyurethane with

a NCO/OH ratio of 1.2. Since the ^2H longitudinal relaxation was found to be nonexponential, we have used a stretched exponential equation of the type Kohlrausch−Williams−Watts to determine the value of T_{1ww}. With the help of the gamma function as well as the values of T_{1ww} and of the stretch parameter β, we were able to determine the average value of T_1 $\langle T_1 \rangle$ without knowing the shape of its distribution function. The study of ^2H NMR T_1 as a function of temperature has shown the potential of this technique to monitor the changes in molecular dynamics during the aging process. Aging the sample with a NCO/OH ratio of 1.4 at ambient conditions for 1 year and by the accelerated treatment for 7 months (at 80 °C) resulted in a similar variation of the $\langle T_1 \rangle$ values, which suggests that similar aging processes occurred for both treatments. However, the use of the β factor showed that the aging processes were indeed different, with a broader distribution of the structure (smaller value of β) in the case of the accelerated aging process. Thus, the application of monitoring the stretch parameter β as a function of temperature and time is complementary to relaxation time measurements and provides further insight into the degradation of the sample.

Acknowledgment. The authors thank Ms. N. Gagnon for the synthesis of the polymers. This research was supported by Department of National Defence of Canada, the Natural Sciences and Engineering Research Council of Canada, and the Fonds pour la Formation de Chercheurs et l'Aide à la Recherche (FCAR) from the Province of Québec.

References and Notes

(1) (a) Muthiah, R.; Varghese, T. L.; Ninan, K. N.; Krishnamusthy, V. N. *Propellants, Explos., Pyrotech.* **1998**, *23*, 90. (b) Tokui, H.; Saitoh, T.; Hori, K.; Notono, K.; Iwama, A. 21th International Annual Conference of ICT, Technology of Polymer Compounds and Energetic Materials, Institut fur Chemische Technology, Karlsruhe, Germany, July 3−July 6, ISSN 0722-4087, 1990, 7-1.

(2) Davenas, A.; Lucas, R.; Zeller, B.; Bac, J. P.; Gossant, B.; Prigent, G.; Gondouin, B.; Brunet, J.; Austry, H.; Couturier, R.; Perut, C.; Tanzia, J. M. *Technologie des Propergols Solides*; Masson Editors, 1989; Chapter 10.

(3) (a) Frankel, M. B.; Grant, L. R.; Flanagan, J. E. *J. Propul. Power* **1992**, *8*, 560. (b) Eroglu, M. S.; Güven, O. *J. Appl. Polym. Sci.* **1996**, *60*, 1361. (c) Eroglu, M. S.; Hazer, B.; Güven, O.; Baysal, B. M. *J. Appl. Polym. Sci.* **1996**, *60*, 2141. (d) Eroglu, M. S.; Güven, O. *J. Appl. Polym. Sci.* **1996**, *61*, 201. (e) Bui, V. T.; Ahad, E.; Rheaume, D.; Raymond, M. P. *J. Appl. Polym. Sci.* **1996**, *62*, 27. (f) Oyumi, Y.; Kimura, E.; Nagayama, K. *Propellants, Explos., Pyrotech.* **1997**, *22*, 263. (g) Pfeil, A.; Löbbecke, S. *Propellants, Explos., Pyrotech.* **1997**, *22*, 137. (h) Kubota, N.; Sonobe, T. *Propellants, Explos., Pyrotech.* **1988**, *13*, 172.

(4) Stacer, R. G.; Husband, D. M. *Propellants, Explos., Pyrotech.* **1991**, *16*, 167.

(5) (a) Menke, K.; Böhnlein-Mauss; Schubert, H. *Propellants, Explos., Pyrotech.* **1996**, *21*, 139. (b) Menke, K.; Eisele, S. *Propellants, Explos., Pyrotech.* **1997**, *22*, 112. (c) Hori, K.; Kimura, M. *Propellants, Explos., Pyrotech.* **1996**, *21*, 160. (d) Nagayama, K.; Oyumi, Y. *Propellants, Explos., Pyrotech.* **1996**, *21*, 74. (e) Oyumi, Y. *Propellants, Explos., Pyrotech.* **1995**, *20*, 150. (f) Oyumi, Y.; Kimura, E. *Propellants, Explos., Pyrotech.* **1996**, *21*, 271. (g) Oyumi, Y.; Nagayama, K. *J. Ener. Mater.* **1997**, *15*, 59. (h) Hori, K.; Kimura, M. *Propellants, Explos., Pyrotech.* **1996**, *21*, 160.

(6) (a) Désilets, S.; Perreault, F. *J. Energ. Mater.* **1997**, *15*, 109. (b) Perreault, F.; Benchabane, M. *Propellants, Explos., Pyrotech.* **1997**, *22*, 193. (c) Bunyan, P.; Cunliffe, A. V.; Davis, A.; Kirby, F. A. *Polym. Degradat. Stabil.* **1993**, *40*, 239. (d) Judge, M. D. *Propellants, Explos., Pyrotech.* **1997**, *22*, 11.

(7) (a) Grosset, C.; Cantin, D.; Villet, A.; Alary, J. *Talanta* **1990**, *37*, 301. (b) Brandšteterova, E.; Štubna, M.; Lehotay, J.; Derneschova, D. *J. Chromatogr.* **1991**, *545*, 205. (c) Francis, V. C.; Sharma, Y. N.; Bhardwaj, I. S. *Angew. Makromol. Chem.* **1983**, *113*, 219. (d) Sreenivasan, K. *Chromatography* **1991**, *32*, 285.

(8) (a) Glatkowski, P. J.; Druy, M. A.; Stevenson, W. A. *Proc. SPIE* **1994**, *2072*, 109. (b) Wernstahl, K. M. *Polym. Mater. Sci. Eng.* **1993**, *68*, 146. (c) Wernstahl, K. M. *Surf. Coat.* **1997**, *80*, 560.

(9) (a) Khan, M. B. *Polym.-Plast. Technol. Eng.* **1993**, *32*, 467. (b) Trong-Ming, D.; Chiu, W. Y.; Hsieh, K. H. *J. Appl. Polym. Sci.* **1991**, *43*, 2193. (c) Chiu, W. Y.; Ding, D. K.; Chen, C. C. *J. Appl. Polym. Sci.* **1991**, *43*, 2175. (d) Suzuki, A.; Ban, M.; Hattori, T.; Akasaka, N.; Matsuda, Y. *Proc. 45th Int. Wire Cabla Symp.* **1996**, 471.

(10) (a) Huang, S., L.; Lai, J. Y. *J. Appl. Polym. Sci.* **1995**, *58*, 1913. (b) Akbas, A.; Aksoy, S.; Hasirci, N. *Polymer* **1994**, *35*, 2568. (c) Flandrin, F. R.; Widmaier, J. M.; Flat, J. J. *Polym. Degradat. Stabil.* **1997**, *57*, 59. (d) Deng, Y. W.; Yu, T. L.; Ho, C. H. *Polym. J.* **1994**, *26*, 1368.

(11) (a) Benchabane, M. *J. Energ. Mater.* **1993**, *11*, 89. (b) Benchabane, M. *J. Energ. Mater.* **1993**, *11*, 101. (c) Benchabane, M. *J. Energ. Mater.* **1993**, *11*, 119.

(12) (a) Drouet-Fleurizelle, L.; Gillereau, D.; Lacabanne, C. *Thermochim. Acta* **1993**, *226*, 43. (b) Sibony-Chaouat, S.; Narkis, M. *Polym. Eng. Sci.* **1985**, *25*, 318. (c) Zhou, P.; Frisch, H. L. *J. Polym. Sci., Part A: Polym. Chem.* **1993**, *31*, 3479. (d) Sartor, G.; Mayer, E.; Johari, G. P. *J. Polym. Sci., Part A: Polym. Chem.* **1994**, *32*, 683.

(13) (a) Zhang, Y.; Shang, S.; Zhang, X.; Wang, D.; Hourston, D. J. *J. Appl. Polym. Sci.* **1995**, *58*, 1803. (b) Parida, D.; Nayak, P.; Mishra, D. K.; Lenka, S.; Nayak, P. L.; Mohanty, S.; Rao, K. K. *J. Appl. Polym. Sci.* **1995**, *56*, 1731. (c) Zhang, Y.; Shang, S.; Zhang, X.; Wang, D.; Houston, D. J. *J. Appl. Polym. Sci.* **1996**, *59*, 1167.

(14) (a) Svensson, L. G. *J. Therm. Anal.* **1997**, *49*, 1017. (b) Chin, A.; Allison, S.; *Proc. 20th Int. Pyrotech. Semin.* **1994**, 203.

(15) (a) Ho, S. Y. *J. Mater. Sci.* **1997**, *32*, 5155. (b) Apicella, A.; D'Amore, A.; Mensitieri, G.; Nicolais, L. *Plas. Rubber Compos. Process Appl.* **1992**, *18*, 127. (c) Ding, J.; Xue, G.; Yang, C.; Chen, R. *J. Appl. Polym. Sci.* **1992**, *45*, 1087.

(16) (a) Buchman, A.; Holdengraber, Y.; Dodiuk, H.; Kenig, S. *Polym. Adv. Technol.* **1991**, *2*, 137. (b) Nakamae, K.; Yamaguchi, K.; Asaoka, S.; Karube, Y.; Sudaryanto *Int. J. Adhesion Adhesives* **1996**, *16*, 277. (c) Bualek, S. *J. Sci. Soc. Thailand* **1983**, *9*, 191.

(17) Kohlrausch, *Ann. Phys. (Leipzig)* **1847**, *12*, 393.

(18) (a) Williams, G.; Fournier, J. *J. Chem. Phys.* **1996**, *104*, 5690. (b) Williams, G.; Watts, D. C. *Trans. Faraday Soc.* **1970**, *66*, 80. (c) Alaimo, M. H.; Roberts, J. E. *Solid State Nucl. Magn. Reson.* **1997**, *8*, 241.

(19) Schmidt-Rohr, K.; Spiess, H. W. *Multidimensional Solid-State NMR and Polymers*, Academic Press: London, 1994.

(20) Lindsey, C. P.; Patterson, G. D. *J. Chem. Phys.* **1980**, *73*, 3348.

(21) (a) Davidson, D. W.; Cole, R. H. *J. Chem. Phys.* **1951**, *19*, 1417. (b) Kaplan, J. I.; Garroway, A. N. *J. Magn. Reson.* **1982**, *49*, 464. (c) Donth, E. J. *Relaxation and Thermodynamics in Polymers: Glass Transition*; Akademie Verlag: Berlin, 1992.

(22) (a) McCrum, N. G.; Read, B. E.; Williams, G. *Anelastic and Dielectric Effects in Polymeric Solids*; Dover: New York, 1991. (b) Williams, G. *Comprehensive Polymer Science*; Allen, G., Bevington, J. C., Eds.; Pergamon: Oxford, 1989; Vol. 2, Chapter 78.

(23) (a) Narayanan, A.; Hartman, J. S.; Bain, A. D. *J. Magn. Reson.* **1995**, *112*, 58. (b) Schnauss, W.; Fujara, F.; Hartmann, K.; Sillescu, H. *Chem. Phys. Lett.* **1990**, *166*, 381.

(24) Désilets, S.; Villeneuve, S.; Laviolette, M.; Auger, M. *J. Polym. Sci., Part A: Polym. Chem.* **1997**, *35*, 2991.

(25) (a) Stejskal, E. O.; Schaefer, J.; Sefcik, M. D.; Mckay, R. A. *Macromolecules* **1981**, *14*, 275. (b) Stejskal, E. O.; Schaefer, J.; Waugh, J. *Magn. Reson.* **1977**, *30*, 287.

(26) Davis, J. H.; Jeffrey, K.; Bloom, M.; Valic, M. I.; Higgs, T. P. *Chem. Phys. Lett.* **1976**, *42*, 390.

(27) (a) Jelinski, L. W. *Annu. Rev. Mater. Sci.* **1985**, *15*, 359. (b) Bovey, F. A., Jelinski, L. W. *J. Phys. Chem.* **1985**, *89*, 571. (c) Abragam, A. *The Principles of Nuclear Magnetism*; Oxford University Press: London, 1961. (d) Slichter, C. P. *Principles of Magnetic Resonance*; Springer-Verlag: Berlin, 1990.

(28) Villeneuve S. Defence Research Establishment Valcartier, unpublished results.
(29) (a) Gajewski, V. *Rubber World* **1990**, *202*, 15. (b) Gajewski, V. *Proceeding. SPI Annual Polyurethane Technical Meeting, Marketing Conference*, Sept 30−Oct 3 1990, p 506. (c) Widmaier, J. M.; Balmer, J. P.; Meyer, G. C. *Polym. Mater. Sci. Eng.* **1987**, *56*, 96.

MA981388+